Nonlinear Electron and Spin Transport in Semiconductor Superlattices

L.L. Bonilla[1], L. Barletti[2] and M. Alvaro[1]

[1] G. Millán Institute of Fluid Dynamics, Nanoscience & Industrial Mathematics, Universidad Carlos III, Leganés, Spain, bonilla@ing.uc3m.es, barletti@math.unifi.it

[2] Dipartimento di Matematica "Ulisse Dini", Università di Firenze, Italy, mariano.alvaro@uc3m.es

Summary. Nonlinear charge transport in strongly coupled semiconductor superlattices is described by two-miniband Wigner–Poisson kinetic equations with BGK collision terms. The hyperbolic limit, in which the collision frequencies are of the same order as the Bloch frequencies due to the electric field, is investigated by means of the Chapman–Enskog perturbation technique, leading to nonlinear drift-diffusion equations for the two miniband populations. In the case of a lateral superlattice with spin-orbit interaction, the corresponding drift-diffusion equations are used to calculate spin-polarized currents and electron spin polarization.

1 Introduction

Semiconductor superlattices are essential ingredients in fast nanoscale oscillators, quantum cascade lasers and infrared detectors. A superlattice (SL) is a quasi-one-dimensional crystal originally proposed by Esaki and Tsu to observe Bloch oscillations, i.e., the periodic coherent motion of electrons in a miniband when an electric field is applied. Once the materials were grown, many interesting nonlinear phenomena were observed, such as self-oscillations of the current through the SL due to charge dipole motion, multistability of stationary charge and field profiles, etc. See the review [1].

Nonlinear charge transport in SLs has been widely studied in the last decade using balance equations for electron densities and electric field. These equations are either proposed using phenomenological arguments or derived ad hoc from kinetic theories [1]. Systematic derivations are scarce. For a single-miniband SL, the Chapman–Enskog (CE) method applied to a semiclassical Boltzmann–Poisson system whose collision term is of Bhatnagar–Gross–Krook (BGK) type yields a generalized drift-diffusion equation (GDDE) [2], and a quantum drift-diffusion equation (QDDE) when applied to a Wigner–Poisson–BGK (WPBGK) system [3]. The quantum WPBGK system contains two pseudo-differential operators, involving the band dispersion relation and the electric potential. The leading order approximation in the hyperbolic limit

A.D. Fitt et al. (eds.), *Progress in Industrial Mathematics at ECMI 2008*,
Mathematics in Industry 15, DOI 10.1007/978-3-642-12110-4_16,

balances collisions and electric potential, and its solution is not obvious because the potential is an a priori unknown solution of the Poisson equation. SLs are simpler because their Wigner functions are periodic in the reciprocal lattice, the potential terms become multiplication operators in Fourier space, and the leading order approximation is straightforward to solve [3].

For sufficiently high applied electric fields, electrons may populate higher minibands, then be scattered to the lowest, etc. Moreover, SLs with diluted magnetic impurities subject to a magnetic field may present spin polarization effects whose understanding is crucial to develop spintronic devices [4]. Even without magnetic impurities, spin polarization could appear due to Rashba spin-orbit interaction [5]. Once we consider electron spin, each miniband is split in two and single-miniband SLs become two-miniband SLs. We shall systematically derive quantum balance equations by the CE method.

2 Wigner Description of a Two-Miniband Superlattice

We shall consider a 2×2 Hamiltonian $\mathbf{H}(x, -i\partial/\partial x)$, in which

$$\begin{aligned} \mathbf{H}(x,k) &= [h_0(k) - eW(x)]\boldsymbol{\sigma}_0 + \mathbf{h}(k)\cdot\boldsymbol{\sigma}] \\ &\equiv \begin{pmatrix} (\alpha+\gamma)(1-\cos kl) - eW(x) + g & -i\beta\sin kl \\ i\beta\sin kl & (\alpha-\gamma)(1-\cos kl) - eW(x) - g \end{pmatrix}. \end{aligned} \tag{1}$$

Then $h_0 = \alpha(1-\cos kl)$, $h_1 = 0$, $h_2 = \beta\sin kl$, $h_3 = \gamma(1-\cos kl) + g$, and

$$\boldsymbol{\sigma}_0 = \begin{pmatrix} 1 & 0 \\ 0 & 1 \end{pmatrix},\ \boldsymbol{\sigma}_1 = \begin{pmatrix} 0 & 1 \\ 1 & 0 \end{pmatrix},\ \boldsymbol{\sigma}_2 = \begin{pmatrix} 0 & -i \\ i & 0 \end{pmatrix},\ \boldsymbol{\sigma}_3 = \begin{pmatrix} 1 & 0 \\ 0 & -1 \end{pmatrix}. \tag{2}$$

The Hamiltonian (1) corresponds to the simplest 2×2 Kane model in which the quadratic and linear terms $(kl)^2/2$ and kl are replaced by $(1-\cos kl)$ and $\sin kl$, respectively. For a SL with two minibands, $2g$ is the miniband gap and $\alpha = (\Delta_1 + \Delta_2)/4$ and $\gamma = (\Delta_1 - \Delta_2)/4$, provided Δ_1 and Δ_2 are the miniband widths. In the case of a lateral SL, $g = \gamma = 0$, and $h_2\boldsymbol{\sigma}_2$ corresponds to the precession term in the Rashba spin-orbit interaction [5]. The other term, the intersubband coupling, depends on the momentum in the y direction and we have not included it here. Small modifications of (1) represent a single miniband SL with dilute magnetic impurities in the presence of a magnetic field B: $g = \gamma = h_2 = 0$, and $h_1 = \beta(B)$ [4]. As in the case of a single miniband SL, $W(x)$ is the electric potential.

The energy minibands $\mathcal{E}^{\pm}(k)$ are the eigenvalues of the free Hamiltonian $\mathbf{H}_0(k) = h_0(k)\boldsymbol{\sigma}_0 + \mathbf{h}(k)\cdot\boldsymbol{\sigma}$ and are given by

$$\mathcal{E}^{\pm}(k) = h_0(k) \pm |\mathbf{h}(k)|. \tag{3}$$

The corresponding spectral projections are $\mathbf{P}^{\pm}(k) = (\boldsymbol{\sigma}_0 \pm \boldsymbol{\nu}(k)\cdot\boldsymbol{\sigma})/2$, with $\boldsymbol{\nu} = \mathbf{h}/|\mathbf{h}(k)|$, so that we can write $\mathbf{H}_0(k) = \mathcal{E}^+(k)\mathbf{P}^+(k) + \mathcal{E}^-(k)\mathbf{P}^-(k)$.

We shall now write the WPBGK equations for the Wigner matrix written in terms of the Pauli matrices $\boldsymbol{\sigma}_s$:

$$\mathbf{f}(x,k,t) = \sum_{s=0}^{3} f^s(x,k,t)\boldsymbol{\sigma}_s = f^0(x,k,t)\boldsymbol{\sigma}_0 + \mathbf{f}(x,k,t)\cdot\boldsymbol{\sigma}. \tag{4}$$

The Wigner components are real and can be related to the coefficients of the Hermitian Wigner matrix by $f_{11} = f^0 + f^3$, $f_{12} = f^1 - if^2$, $f_{21} = f^1 + if^2$, $f_{22} = f^0 - f^3$. The populations of the minibands with energies $\mathcal{E}^{\pm}$ are the moments:

$$n^{\pm}(x,t) = \frac{l}{2\pi}\int_{-\pi/l}^{\pi/l}\left[f^0(x,k,t) \pm \boldsymbol{\nu}\cdot\mathbf{f}(x,k,t)\right]\,dk, \tag{5}$$

and the total electron density is $n^+ + n^-$.

We shall restrict ourselves to the Rashba case, $g = \gamma = h_3 = 0$, from now on. Then $\boldsymbol{\nu} = (0,1,0)$ and $n^{\pm}$ are the densities of electrons having spin $\pm$. After some algebra, we can obtain the following WPBGK equations for the Wigner components

$$\frac{\partial f^0}{\partial t} + \frac{\alpha}{\hbar}\sin kl\,\Delta^- f^0 + \frac{\beta\cos kl}{\hbar}\,\Delta^- f^2 - \Theta f^0 = Q^0[f], \tag{6}$$

$$\frac{\partial \mathbf{f}}{\partial t} + \frac{\alpha \sin kl}{\hbar}\Delta^-\mathbf{f} + \frac{\beta}{\hbar}[\boldsymbol{\nu}\Delta^- f^0\cos kl + \Delta^+(\boldsymbol{\nu}\times\mathbf{f})\sin kl]$$
$$-\Theta\mathbf{f} = \mathbf{Q}[f], \tag{7}$$

$$\varepsilon\,\frac{\partial^2 W}{\partial x^2} = \frac{e}{l}\,(n^+ + n^- - N_D), \tag{8}$$

$$\Theta f^s(x,k,t) = \sum_{j=-\infty}^{\infty}\frac{ejl}{i\hbar}\langle F(x,t)\rangle_j e^{ijkl} f^s_j(x,t), \tag{9}$$

where we have put $f^s(x,k,t) = \sum_{j=-\infty}^{\infty} f^s_j(x,t)\,e^{ijkl}$ and

$$\langle u\rangle_j(x,t) = \frac{1}{jl}\int_{-jl/2}^{jl/2} u(x+s,t)\,ds.$$

Our collision model contains two terms: a BGK term which tries to send $f^0 \pm \boldsymbol{\nu}\cdot\mathbf{f}$ to its (collision-broadened) Fermi–Dirac local equilibrium, and a scattering term which tries to equalize n^+ and n^- [4]:

$$Q^0[f] = -\frac{f^0 - \Omega^0}{\tau}, \quad \mathbf{Q}[f] = -\frac{\mathbf{f}-\boldsymbol{\Omega}}{\tau} - \frac{\mathbf{f}}{\tau_{\mathrm{sc}}}, \tag{10}$$

$$\Omega^0 = \frac{\phi^+ + \phi^-}{2}, \quad \boldsymbol{\Omega} = \frac{\phi^+ - \phi^-}{2}\,\boldsymbol{\nu}, \tag{11}$$

where (see [6] for details and [7] for the numerical method employed)

$$\phi^{\pm}(k;\mu^{\pm}) = \int_{-\infty}^{+\infty} \frac{D_\Gamma\left(E-\mathcal{E}^{\pm}(k)\right)}{1+\exp\left(\frac{E-\mu^{\pm}}{k_B T}\right)}\, dE \tag{12}$$

$$D_\Gamma(E) = \frac{\sqrt{2m^*}}{2\pi\hbar L_z}\int_0^{\infty} \frac{\delta_\Gamma(E_y+E_1-E)}{\sqrt{E_y}}\, dE_y, \quad \delta_\Gamma(E) = \frac{\sqrt{2}\,\Gamma^3/\pi}{\Gamma^4+E^4} \tag{13}$$

$$\frac{l}{2\pi}\int_{-\pi/l}^{\pi/l} \phi^{\pm}(k;n^{\pm})\, dk = n^{\pm}. \tag{14}$$

In (12), $\mu^{\pm} = \mu^{\pm}(n^{\pm})$ solve (14). Our collision model satisfies charge continuity. In fact, from (6) to (8) we obtain:

$$\frac{\partial}{\partial t}(n^+ + n^-) + \Delta^-\left[\frac{l}{\pi\hbar}\int_{-\pi/l}^{\pi/l} (\alpha\,\sin kl\, f^0 + \beta\,\cos kl\, f^2)\, dk\right] = 0. \tag{15}$$

Since $\Delta^- u(x) = l\,\partial\langle u(x)\rangle_1/\partial x$, (15) provides charge continuity. From (8) and (15), we get Ampère's law ($J(t)$ is the total current density):

$$\varepsilon\frac{\partial F}{\partial t} + \left\langle \frac{el}{\pi\hbar}\int_{-\pi/l}^{\pi/l} (\alpha\,\sin kl\, f^0 + \beta\,\cos kl\, f^2)\, dk \right\rangle_1 = J(t). \tag{16}$$

3 Quantum Drift-Diffusion Equations with Spin-Orbit Interaction

In the simpler case of a lateral SL with the precession term of Rashba spin-orbit interaction (but no intersubband coupling), we can obtain explicit rate equations for $n^{\pm}$ by means of the CE method. First of all, we should decide the order of magnitude of the terms in the WPBGK equations (6) and (7) in the hyperbolic limit. In this limit, the collision frequency $1/\tau$ and the Bloch frequency $eF_M l/\hbar$ are of the same order, and the scattering time $\tau_{\rm sc}$ is much longer than the collision time τ. Then, a suitable small parameter λ can be introduced [2] such that the scaled Wigner equations read as follows:

$$\lambda\frac{\partial f^0}{\partial t} + \lambda\frac{\alpha}{\hbar}\sin kl\,\Delta^- f^0 + \lambda\frac{\beta\cos kl}{\hbar}\,\Delta^- f^2 - \Theta f^0 = Q^0[f], \tag{17}$$

$$\lambda\frac{\partial \mathbf{f}}{\partial t} + \lambda\frac{\alpha\sin kl}{\hbar}\Delta^-\mathbf{f} + \lambda\frac{\beta}{\hbar}[\boldsymbol{\nu}\Delta^- f^0\cos kl + \Delta^+(\boldsymbol{\nu}\times\mathbf{f})\sin kl] \tag{18}$$

$$-\Theta\mathbf{f} = -\frac{\mathbf{f}-\boldsymbol{\Omega}}{\tau} - \lambda\frac{\mathbf{f}}{\tau_{\rm sc}}, \tag{19}$$

To derive the reduced balance equations, we use the following CE ansatz:

$$f(x,k,t;\lambda) = f^{(0)}(k;n^+,n^-,F) + \sum_{m=1}^{\infty} f^{(m)}(k;n^+,n^-,F)\,\lambda^m, \tag{20}$$

$$\varepsilon\frac{\partial F}{\partial t} + \sum_{m=0}^{\infty} J_m(n^+,n^-,F)\,\lambda^m = J(t), \quad \frac{\partial n^\pm}{\partial t} = \sum_{m=0}^{\infty} A_m^\pm(n^+,n^-,F)\,\lambda^m. \tag{21}$$

$A_m^\pm$ and J_m are related through the Poisson equation (8), so that

$$A_m^+ + A_m^- = -\frac{l}{e}\,\frac{\partial J_m}{\partial x}. \tag{22}$$

Following the CE procedure up to order 2 (see [6] for details) we obtain

$$\frac{\partial n^\pm}{\partial t} + \Delta^- D_\pm(n^+,n^-,F) = \mp R(n^+,n^-,F), \tag{23}$$

$$\varepsilon\,\frac{\partial F}{\partial t} + e\,\langle D_+ + D_-\rangle_1 = J, \tag{24}$$

$$D_\pm = -\frac{\alpha}{\hbar}\,\mathrm{Im}(\varphi_1^0 \pm \varphi_1^2 + \psi_1^0 \pm \psi_1^2) \pm \frac{\beta}{\hbar}\,\mathrm{Re}(\varphi_1^0 \pm \varphi_1^2 + \psi_1^0 \pm \psi_1^2), \tag{25}$$

$$R = \frac{n^+ - n^-\theta(\mu^- \mathcal{E}^+_{\min})}{\tau_{sc}}. \tag{26}$$

Here, $\varphi \equiv f^{(0)}$ and $\psi \equiv f^{(1)}$ can be explicitly calculated and yield

$$\begin{aligned}
D_\pm = {} & \frac{(\alpha\vartheta_1 \pm \beta)\phi_1^\pm}{\hbar\,(1+\vartheta_1^2)} \mp \frac{\tau\,(\phi_1^+ - \phi_1^-)\,[2\alpha\vartheta_1 \pm \beta(1-\vartheta_1^2)]}{2\hbar\tau_{\mathrm{sc}}(1+\vartheta_1^2)^2} \\
& + \frac{[2\alpha\vartheta_1 \pm \beta(1-\vartheta_1^2)]\,\alpha\tau}{\hbar^2\,(1+\vartheta_1^2)^2}\,\frac{\partial\phi_1^\pm}{\partial n^\pm}\left[\Delta^-\left(\frac{\alpha\vartheta_1 \pm \beta}{\hbar\,(1+\vartheta_1^2)}\phi_1^\pm\right) \pm \frac{\hbar}{\alpha\tau_{sc}}(n^+ - n^-)\right] \\
& + \frac{\alpha\,(3\vartheta_1^2 - 1) \pm \beta\vartheta_1(3-\vartheta_1^2)}{\hbar(1+\vartheta_1^2)^3}\,\frac{l\tau^2\phi_1^\pm}{\hbar\varepsilon}\left(\frac{J}{e} - \left\langle\left\langle\frac{\alpha\,(\phi_1^+ + \phi_1^-)\vartheta_1}{\hbar(1+\vartheta_1^2)}\right\rangle_1\right\rangle_1\right. \\
& \left. - \left\langle\left\langle\frac{\beta\,(\phi_1^+ - \phi_1^-)}{\hbar(1+\vartheta_1^2)}\right\rangle_1\right\rangle_1\right) - \frac{(\alpha^2+\beta^2)\tau}{2\hbar^2(1+\vartheta_1^2)}\,\Delta^- n^\pm \\
& + \frac{\tau}{2\hbar^2(1+\vartheta_1^2)}\left[(\alpha^2 - \beta^2 \mp 2\alpha\beta\vartheta_1)\,\Delta^-\left(\frac{\phi_2^\pm}{1+\vartheta_2^2}\right)\right. \\
& \left. + [(\beta^2-\alpha^2)\vartheta_1 \mp 2\alpha\beta]\,\Delta^-\left(\frac{\vartheta_2\phi_2^\pm}{1+\vartheta_2^2}\right)\right],
\end{aligned} \tag{27}$$

where $\phi_j^\pm$ are the Fourier components of the local Fermi–Dirac equilibrium functions (12) and $\vartheta_j \equiv \frac{\tau e j l}{\hbar}\,\langle F\rangle_j$.

The simulations shown below are based on the quantum drift-diffusion equations (23)–(27). Figure 1a shows electric current vs. field in a spatially uniform stationary state, for a Fermi–Dirac statistics, for different values of the level broadening parameter Γ, and for the Botzmann statistics without

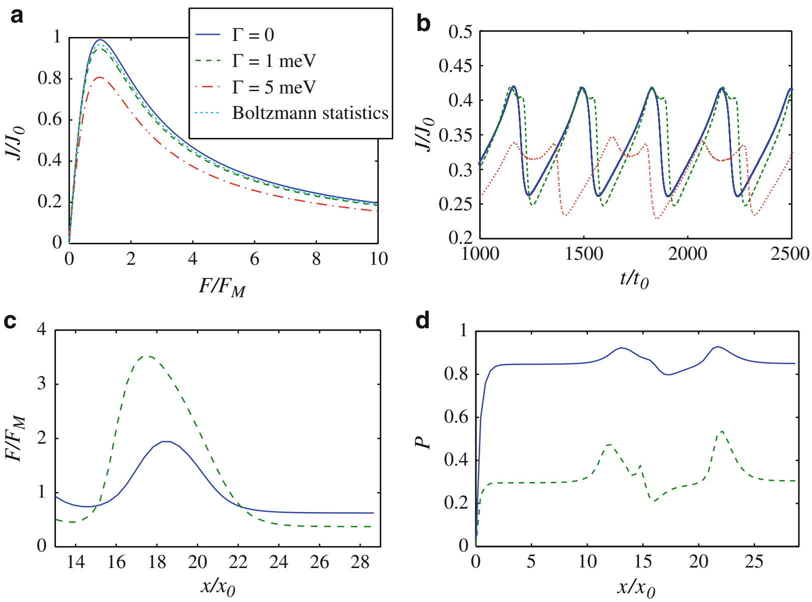

Fig. 1. Electric current vs. field in the stationary case (**a**). Total current vs. time (**b**), electric field profile (**c**) and polarization profile (**d**) during current self-oscillations

broadening. Figures 1b–1d illustrate (for different values of Γ and also for the Botzmann case), a non-stationary behavior showing stable, self-sustained current and spin oscillations. They are due to the periodic formation of a pulse of the electric field at the cathode $x = 0$ and its motion through the superlattice. Plot (b) is total current density vs. time while (c) and (d) show the electric field (c) and spin polarization (d) profiles during current self-oscillations. We have used the following values of the parameters: $\alpha = 8\,\text{meV}$, $\beta = 2.63\,\text{meV}$, $L_z = 3.1\,\text{nm}$, $T = 5\,\text{K}$, $\tau = 5.56\times 10^{-14}\,\text{s}$, $\tau_{\text{sc}} = 5.56\times 10^{-13}\,\text{s}$, $N_D = 4.048\times 10^{10}\,\text{cm}^{-2}$, $m^* = 0.0992$, $V = 3\,\text{V}$. The plot units are the following: $F_M = 23.42\,\text{kV/cm}$, $x_0 = 19.4\,\text{nm}$, $t_0 = 0.082\,\text{ps}$, $J_0 = 3.94\times 10^4\text{A/cm}^2$.

References

1. Bonilla, L.L., Grahn, H.T.: Rep. Prog. Phys. **68**, 577 (2005)
2. Bonilla, L.L., Escobedo, R., Perales, A.: Phys. Rev. B **68**, 241304(R) (2003)
3. Bonilla, L.L., Escobedo, R.: Math. Mod. Meth. Appl. Sci. **15**(8), 1253 (2005)
4. Sánchez, D., MacDonald, A.H., Platero, G.: Phys. Rev. B **65**, 035301 (2002)
5. Kleinert, P., Bryksin, V.V., Bleibaum, O.: Phys. Rev. B **72**, 195311 (2005)
6. Bonilla, L.L., Barletti, L., Alvaro, M.: SIAM J. Appl. Math. **69**(2), 494–513 (2008)